A. G. Dewey
J. D. Crow

The Application of GaAlAs Lasers to High-Resolution Liquid-Crystal Projection Displays

In this review we describe a high-resolution liquid-crystal (LC) display that uses multiple GaAlAs lasers to write on the LC cell. Arrays of high-powered lasers were needed to meet the writing speed requirements of the display. A fiber optic delivery system was developed to allow high-resolution, multi-spot writing on the cell, regardless of the laser configuration used. The flexibility and unconstrained length of the fiber optics also permitted simplification in the design of the scanner system which moved the optical beams over the LC cell. Because of the proximity of the injection laser's wavelength to the visible spectrum used in the display projection system, and because of divergence of the beams in the optical delivery system, a reflective LC cell was designed. Almost total absorption of the GaAlAs laser beam was achieved. This paper discusses the thermal and optical properties of the cell and their effect on the writing characteristics and the quality of the projected image (contrast and brightness). An off-axis projection system, which was designed for use with the reflective cell, creates a high-resolution image on the screen.

Introduction

Thermal writing on a smectic liquid-crystal (LC) cell with a scanned laser beam was first reported by Kahn [1] in 1973. Since that time the potential of this technology as a high-information-content projection display with storage and selective erase has been recognized, and several other research groups have done work in this area [2–5]. The LC cell can be written on using either of two approaches, matrix addressing or beam addressing. For large-information-content displays, the matrix-addressed approach suffers from the large number of drivers required and the low yield associated with manufacturing large addressing grids. Most of the beam-addressed work has used a Nd:YAG laser scanned by galvanometer mirrors to write on a transmissive LC cell.

For widespread use of LC cells in high-resolution displays, the GaAlAs injection laser is the preferred writing beam source. The advantages that it has over the Nd:YAG laser are small size, ease of modulation, efficiency in converting electrical energy to optical energy, and the potential for low manufacturing cost. Because the device is planar-processed, either single device chips or monolithic laser arrays can be fabricated at comparable cost. At IBM, both approaches have been studied experimentally. Due to the low yield of monolithic laser arrays which met the requirements of the laser liquid-crystal display (LLCD), this approach was not implemented and is not discussed here.

In order to obtain the writing speed required for the display, more optical power is needed than is available from a single injection laser. A multi-beam approach to writing the cell was used to overcome this limitation, based on a close-packed array of individually driven optical fibers. The spacing between fibers at the sources is arbitrary. The scanning system which moves the multi-spot array over the LC cell takes advantage of the flexibility of the fiber optics, so that a small, simple on-axis writing lens can be used to project the fiber array image onto the cell.

Because the GaAlAs wavelength is close to the visible spectrum needed for projecting the display image, a reflective LC cell has been developed in contrast to the previous transmissive cells [1–4]. Excellent laser energy absorption has been achieved. The reflective cell requires an off-axis projection system, and we describe a design which has demonstrated both good contrast and high brightness. The

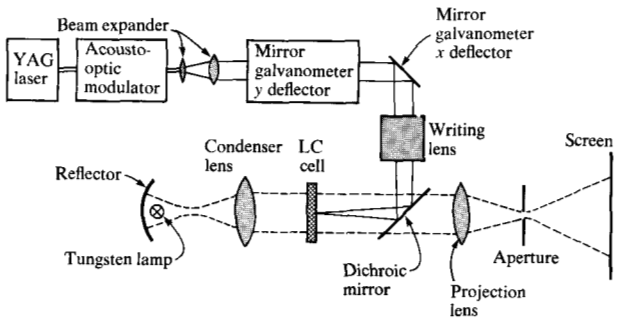

Figure 1 Laser-addressed liquid-crystal display system.

reflective cell uses a smectic liquid crystal which has inherent storage capability, so that the laser need not refresh the information displayed on the screen.

In this review, we discuss the design trade-offs in the development of an experimental liquid-crystal display, particularly in the area of laser power and life, cell addressing methods, and writing speed. We also present results for an eight-laser experimental system, and we project the ultimate limits of the technology for a high-information-content storage display. In discussing the design trade-offs, we assume as requirements for this LLCD a writing speed of 10^6 picture elements (pels) per second, a total number of resolvable pels of at least 2×10^6, a maximum ambient temperature of $\approx$50°C, and a display lifetime of five years.

Laser-addressed smectic LC displays

The early experiments [6] on laser-addressed LC displays used a cholesteric–nematic mixture. Heating the LC with the laser beam created a scattering texture which could subsequently be erased by aligning the LC with an electric field. It was later discovered [1] that a smectic LC gave improved image quality (contrast and resolution) and permanent storage of the written information as long as the LC was held in the smectic state. The image could not be erased by electric field alone, but it could be erased by heating to the isotropic state and cooling slowly, or by cooling rapidly in the presence of a field. This property of the smectic cell provides a useful addition to the capability of the display system, namely selective erasure. Since the applied field has no effect on information stored on the cell, it can be applied while the laser beam is being rescanned over a previously written area. This area subsequently cools, in the presence of the field, to the erased state. More recently, different smectic materials have been discovered [4] which can be erased by a field alone. The selective erase mechanism still works, but with a field which is below the threshold for total erasure.

A schematic of a typical display using a transmissive LC cell, written by a Nd:YAG laser, is shown in Fig. 1. The cell is constructed from two glass substrates coated with a transparent conductor, indium–tin oxide (ITO). The LC thickness of $\approx$12 μm is maintained by a Mylar spacer and the cell is sealed with epoxy. In addition to being used to apply the erase field, the ITO provides the means for absorbing laser energy. By careful control of the conditions under which these ITO coatings were sputtered, it was possible to achieve up to 35% absorption (in each substrate) of the 1.06-μm laser energy while maintaining high transmission of the visible projection light. The minimum size of a written spot on the cell is determined primarily by the size of the laser beam, and to some extent by the thickness of the cell. In Kahn's early work [1] this minimum size was about 20 μm. The spot size is also determined by the amount of energy delivered (power and pulse length), and the maximum size, which is determined by the thermal properties of the cell, may be more than ten times the minimum. The writing speed is given in Ref. [1] as 10^4 spots/s for 20 mW of power, which implies an energy of 2 μJ per spot.

The LC cell is projected onto a screen, at any desired magnification, and gives high-contrast black writing on a white background. Because of the high resolution of the LC cell (up to 100 points/mm) and the fact that there are no hard limitations on the size of the cell, it is possible with a high-quality projection system to achieve a screen resolution (number of resolvable points) which is higher than that of any other display technology. The highest resolution demonstrated to date is $\approx$4000 $\times$ 4000 points using a 15-cm-diameter LC cell [3].

High-power (GaAl)As lasers

• *Laser requirements*

The laser requirements are determined by the energy needed to write the display cell, and by the desire for reliable writing head operation for the life of the display. We can achieve good-contrast writing using a GaAs laser with an energy of $\approx$0.2 μJ/pel for a pel size of 12.5 μm. Assuming that the scanning system will allow writing during 70% of the time, and that the laser power can be delivered to the LC cell with 50% efficiency, a total average laser power of 570 mW is needed for 1-Mpel/s writing. A single semiconductor laser cannot deliver this average laser power, but an array of lasers can. A high-resolution character height has about 24–40 spots, so it is natural to consider linear arrays of spots of this size writing vertically on the display cell while being scanned horizontally across the cell. With a 32-spot array (chosen for compatibility with digital data formats) coming from 32 lasers, we would need $\approx$20 mW per laser. Each laser would deliver 10 mW at the LC cell; thus, a dwell time of 20 μs would be needed for 0.2 μJ/pel of energy.

The "writing" life of the laser can be less than the display life because the LC cell has storage and the display is anticipated to be updated infrequently. We have estimated that ≈500 h would be adequate laser life.

• *Laser structures*

At IBM, lasers of the diffused planar-stripe type have been fabricated for the LLCD application. Compared to an oxide-stripe device, the Zn-diffused p-side contact (typically 15 μm wide) provides current confinement, lowers the threshold current density, and narrows and stabilizes the emission pattern. A short cavity length of 250 μm is used to improve modal stability at high power. The lasers had uncoated facets. The structure and fabrication of these lasers are described in detail in Ref. [7]. This laser's typical output power *vs.* drive current is shown in Fig. 2(a). It is seen to be kink-free up to cw powers of 25 mW. The far-field emission pattern of the laser is shown in Fig. 2(b). The coupling of this laser to fiber lightguides is discussed in the next section.

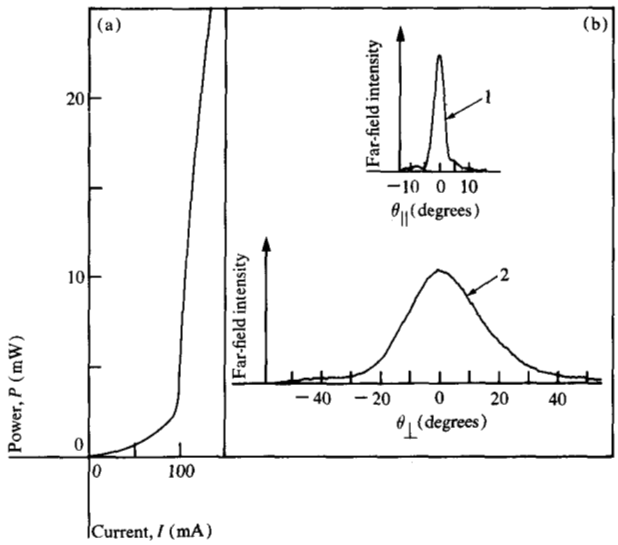

Figure 2 (a) Typical single-facet light output *vs.* drive current for the Zn-diffused stripe laser of Ref. [9]. (b) The far-field optical intensity profiles of the same laser, both in and perpendicular to the plane of the p-n junction.

The reliability of this laser is discussed in Refs. [7, 8]. The devices were aged at 20 mW single-facet output power and room temperature under constant optical power conditions. Laser cumulative failure distributions (failure is the inability to deliver 20 mW of single-facet power) were log normal in time, with median life $\langle t \rangle$ being ≈300 h and a standard deviation $\sigma = 1.8$. Screening tests were developed which eliminated about 70% of the early-failing devices, thus improving $\langle t \rangle$ to ≈1800 h and lowering σ to ≈0.8. In this case, about 5% of the devices did not live the required 500 h. As the LLCD uses arrays of nominally 32 lasers, it is the aggregate reliability of this array which must be considered. For a 32-laser array consisting of screened devices, the array median life $\langle t \rangle_a$ is ≈350 h. Improvements in the life of this device are required to meet LLCD system requirements.

Recent data from H. Imai *et al.* [9] indicate two processing changes which might improve the life of this laser structure: the use of a more stable solder such as AuSn alloy and facet coating of the laser with Al_2O_3. At 70°C, $\langle t \rangle$ for the devices of Ref. [9] was reported as 2000 h, with $\sigma = 1.4$. Using a 0.7-eV thermal activation energy, this extrapolates to a room-temperature median life $\langle t \rangle_{rt}$ of 1.1×10^5 h. An array of 32 of these devices would have $\langle t \rangle_a = 6500$ h [10] ($\sigma = 0.74$). Thus, more than 99% of the arrays could be expected to live the required 500 h. Device screening tests were applied to the lasers of Ref. [9].

Even with the improved lasers of [9], some form of service for lasers in the array might be needed. This servicing could be performed on a routine schedule if each laser were backed up by another laser which was automatically activated if the primary laser were to fail. Ref. [8] indicates that the improvement in effective array life t_e with laser redundancy for each spot is about a factor of ten. More significantly, laser failure does not result in the loss of the spot on the LC cell; thus, with routine servicing it is unlikely that the LLCD system would ever fail as a result of laser failure.

Other device structures which may offer improved beam stability at high power might also be used in the LLCD application. The large-optical-cavity (LOC) structure has recently been incorporated into mode-stable structures to yield high-power, stable lasers [11]. Buried-heterostructure (BH) LOC lasers have demonstrated single-mode behavior up to 20 mW of optical output power [12], and constricted double-heterojunction (CDH) LOC lasers have operated single-mode at 40 mW output power per facet [11]. Another technique to enhance optical output power is to lower the optical power density at the facet by removing the light-confining region near the end facets. Recently, transverse junction stripe devices with the index guiding removed near the facets [13] have demonstrated greater than 15 mW of single-mode power per facet. All these structures are complicated and may be difficult to manufacture.

• *Laser packaging*

The laser package developed at IBM uses a Si wafer containing etched grooves, both as the substrate for the laser array [where an array can be one or more devices in a single (GaAl)As chip] and as a miniature optical bench for the self-registered alignment of the optical components to the laser. This design offers the optimum combination of effi-

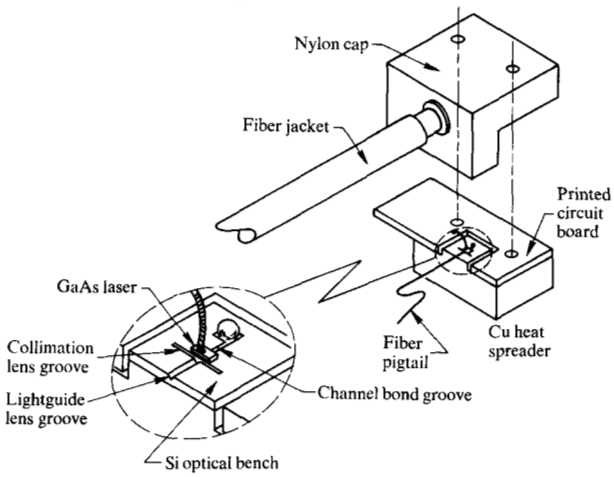

Figure 3 Schematic of the laser package showing the fiber pigtail's protective jacket and strain relief cap, the PC board electrical lead frame, and the Si substrate's Cu heat spreader. The blow-up of the Si substrate indicates the fiber optic component, the laser bonding grooves, and the n-side flying lead.

cient coupling of the laser to the fiber, heat dissipation capability, device isolation in multi-device arrays (both thermal and electrical), and laser bonding quality. It also offers the potential for inexpensive, automated laser package assembly. References [14–16] report early work on this packaging approach, primarily applied to multi-laser arrays. We review here single-laser packages and present some more recent results. The package structure for a single-laser chip is shown in Fig. 3. The single-laser substrate is an etched Si chip, typically 6.4 × 6.4 mm, with evaporated contact metallurgy on both sides. Also shown in the figure are etched grooves for a cylindrical laser collimating lens, and a lightguide, as well as an etched groove and cavity to be used for laser bonding. The dimension of each groove is tailored to its function, yet all are fabricated in a common etching step. The Si substrate is soldered to a Cu heat spreader, which in turn is attached to the laser subassembly (see Fig. 4).

The bonding procedure, developed by Comerford [17], uses the groove under the laser as a capillary to deliver In solder from a remote reservoir to the laser. This bond has less contamination of the In solder and less alloying of the solder with the Au contact metallurgy than previous, predeposited-solder bonding techniques [14]. The process also allows positioning of the laser directly on the Si optical bench surface. This removes a major optical alignment uncertainty in the package, namely the thickness of the solder joint.

Analysis by Laff [15] of the thermal characteristics of laser-on-Si packages predicts a thermal resistance between the laser and heat sink (under the Si) of ≈20°C/W, only 4°C/W larger than expected from an all-Cu-substrate package. This resistance has been experimentally confirmed; in fact, larger variances in the thermal resistance were observed due to bond quality (alloying, contamination, or voids) than to the laser substrate material (Cu or Si). The thermal resistance of the capillary-bonded package is ≈23°C/W [17].

The life of lasers in an ambient temperature of 50°C, even with the lasers of Ref. [9], is inadequate for the LLCD application. Therefore, active cooling to the ambient with thermoelectric coolers backed by fins is used to maintain the junction temperature near 25°C.

Fiber optic delivery system

A unique characteristic of the LLCD is the fiber optic delivery of laser light to the LC cell. This delivery system is shown schematically in Fig. 4. It consists of a piece of fiber which acts as a cylindrical lens to collimate the laser's output beam and make it symmetrical in beamshape and divergence, the transmission fiber, and a small plastic imaging lens. There are attractive features to this approach. Multi-spot arrays can be built from single lasers. This allows optimization of laser yield and reliability which is not possible if a conventional optical lens system is used to image a laser array onto an LC cell. The small size of the fibers allows close and rigid placement of the optics in front of the laser facet. Conventional imaging lens systems are continually plagued with maintaining alignment in systems involving mechanical motion of parts. The flexibility of the fibers allows the use of mechanical scanners to simplify LC cell scanning, as well as the imaging optics. Finally, the low loss of the fibers allows remote placement of the lasers from the LC cell. This permits considerable flexibility in chassis and cooling design.

Because the fibers used are multi-mode, there is a loss of radiance between the coherent laser and the fiber output. The design of the optical delivery system minimizes this loss of radiance in order to maximize the amount of laser power that can be delivered to a small spot on the LC cell, consistent with the alignment and assembly tolerances of the system.

• *Laser-lightguide coupling*

The most critical part of the optical assembly is the coupling of the laser light to the fiber lightguide. Table 1 indicates the tolerances which must be met to couple at least 50% of the light from the laser to the lightguide. The laser beam characteristics of Fig. 2(b) were assumed. The numerical aperture NA of 0.15 is minimal for a fiber with useful flexural and handling characteristics. As the core diameter is decreased, the required accuracy of vertical alignment

Table 1 Required tolerances to couple 50% of the light from the laser to the lightguide.

Core diameter (μm)	*Optimum lens diameter* (μm)	*Maximum misaligment normal to Si surface* (μm)	*Maximum misalignment on Si surface* (μm)
50	70	5	20
40	60	4	14
30	50	3	10
20	40	2	5

increases, as does the required accuracy for placement of the laser on the Si surface. Our design approach was to optimize the fiber core diameter both for ease in laser package fabrication tolerance and for minimal minification in the fiber-to-LC-cell imaging lens. Fibers with core diameter in the 40–50-μm range satisfy both conditions.

As discussed in [14], laser-fiber coupling systems using Si as a common substrate have been routinely fabricated, with 70-μm-diameter cylindrical lenses and 63-μm-core-diameter fibers (graded index, $NA = 0.15$, outer diameter = 125 μm). The maximum theoretical coupling efficiency is about 80%, using lasers with characteristics similar to those of Fig. 2; the experimentally measured efficiency for these early units was consistently >60%. The major sources of misalignment between the optical components were variations in the solder thickness, the fiber lens, or the lightguide diameter. The channel-bonding technique has eliminated the former misalignment, while developments in optical fiber production have reduced fiber-diameter variations to <1%. Therefore, we expect that worst-case misalignment in the 3–4-μm range is feasible, and that 40-μm-core fibers could also be used, if needed.

The fiber pigtail from the laser package is then connected to one of the fibers of a furcated multi-fiber cable of ≈8-mm diameter. The cable, a standard commercially available design, is flexible, lightweight, and easily routed within the display to the scanner head assembly. The multi-laser/cable assembly is shown schematically in Fig. 4.

• *Fiber array scanner*

The fibers used in the experimental LLCD have a diameter of 125 μm, a graded index profile core of 63 μm, and $NA = 0.15$. The laser beam emitted by the end of the fiber has a full-width, half-power diameter of 43 μm. The eight fibers are arranged in two rows in a close-packed structure, as shown in Fig. 4. A dummy fiber is added to the array to help maintain the proper spacing during assembly.

The end of the fiber array is polished flat and forms an array of sources 43 μm in diameter with a vertical spacing of

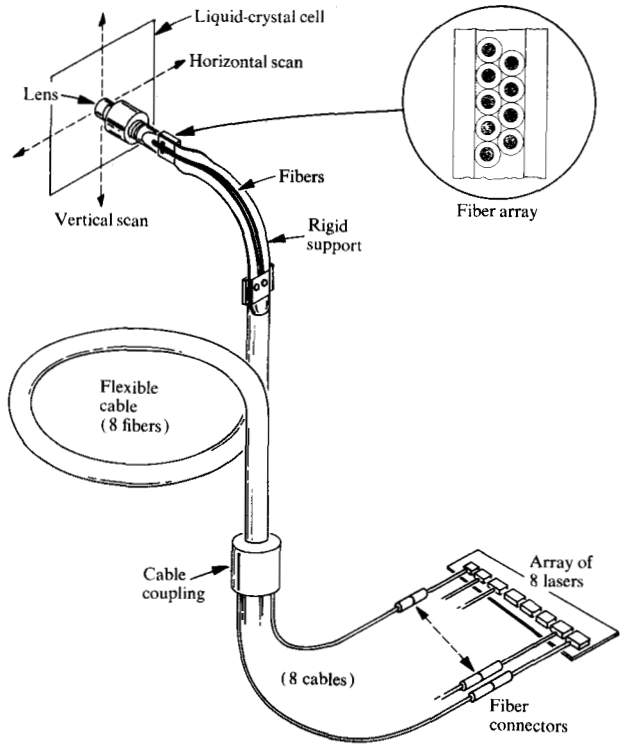

Figure 4 Fiber optic delivery system of the LLCD.

63 μm. The array is imaged onto the LC cell and raster-scanned over the cell. The ability to scan the lens results in a relatively simple lens design. Its field of view is only that of the dimension of the fiber array and it can be made small, lightweight, and inexpensive. The number of spots which can be written on the LC cell is limited only by the range of the linear scanning mechanism, and hence the number of resolvable points on the display is limited only by the resolution limit of the projection lens.

The scanning system must be sufficiently accurate to give acceptable quality in the projected image of the LC cell. As in any raster-scanned system, the scanning speed is vastly different in the two axes. Let us arbitrarily call the fast axis x and the slow axis y. As the head is scanned across the x axis it writes N rows of information, where N is the number of lasers used.

Scanning in the x direction is performed by a voice-coil actuator operated in a linear scanning mode (*i.e.*, with a constant velocity across the scanned field). Figure 5 shows the configuration. Information is written in both scan directions to maximize the writing duty factor. Bidirectional writing requires more complicated buffering and preprocessing of the data to be written, and more than an order-

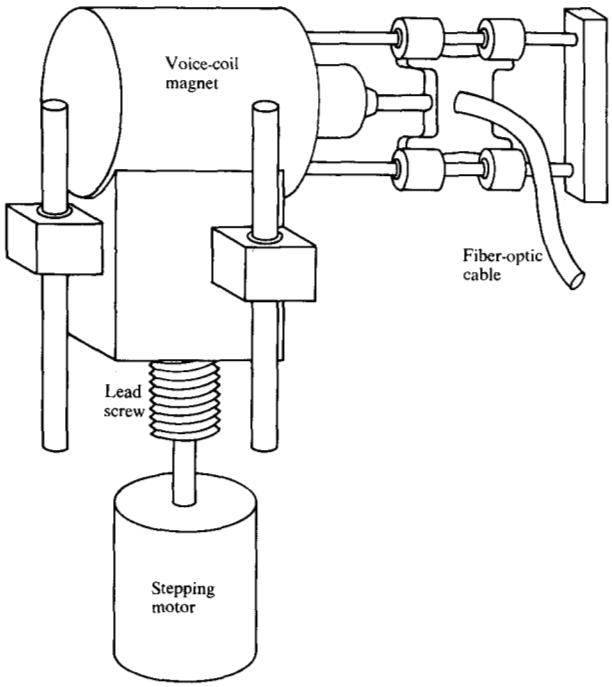

Figure 5 Linear scanning system.

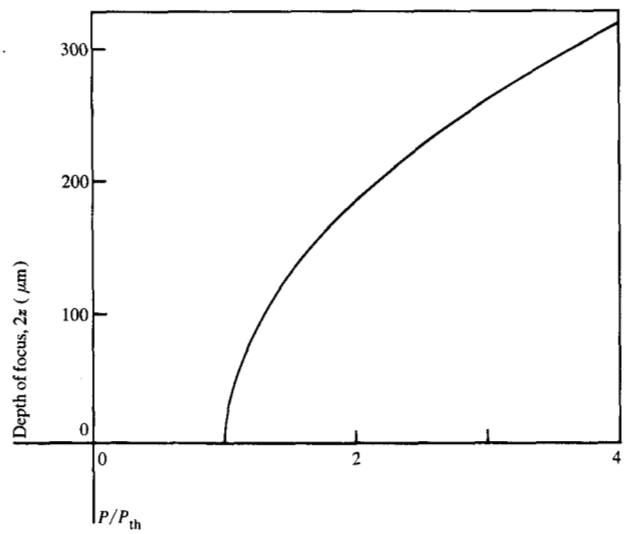

Figure 6 Depth of focus of the LLCD writing lens.

of-magnitude higher accuracy in spot placement than unidirectional writing. Such accuracy can only be achieved by a system which monitors the position of the writing beam itself. In our experimental LLCD, the motion of the writing head is monitored by a linear optical position sensor.

To write a 12.5-μm spot every 20 μs requires an x-scanner velocity of 625 mm/s (25 in./s). To write with a high duty factor, rapid reversals of the scan are required, implying a high deceleration and acceleration of the head (*e.g.*, 2 Gs are required for a turnaround time of 60 ms). Voice-coil actuators can achieve this performance.

For scanning in the y direction, a stepping motor driving a precision lead screw was chosen. This staircase motion is necessary (a) for bidirectional scanning, (b) in order to have the scan lines orthogonal to the y axis, (c) whenever there are enough elements in the write head that the slope of the scan lines becomes noticeable to the viewer, or (d) if the x-scan is asynchronous.

- *Fiber array–LC cell imaging*

The writing lens was designed by R. Tibbetts [18]. It has two elements and is molded from plastic. It has a 7-mm aperture and a focal length of $\approx$5 mm, and it was designed for a demagnification of 3.5, with a focus $NA = 0.5$. As mentioned earlier, the ability to scan this lens over the 25 $\times$ 32-mm LC cell was an important feature in simplying its design, as fixed, full-field designs for multi-laser heads required more than ten elements and were expensive.

Because of the high NA, we had to be concerned about the focal depth of the lens. This could create very tight tolerances on the accuracy with which the linear scanner tracks the LC cell (which itself may have deviations from perfect flatness of several microns). Sincerbox [19] investigated the depth of focus necessary for writing on the cell, including the effects of the optical beam's power profile on thermal writing. Figure 6 shows the results of the calculation for a beam radius of $\sigma = 5$ μm and a wavelength of $\lambda = 0.85$ μm. Note that for power levels of several times threshold, which are necessary for high-contrast writing, the depth of focus is substantial. This depth of focus is compatible with the scanner accuracy and LC cell flatness.

Reflective LC cell

The use of GaAs lasers and a fiber optic delivery system required a redesign of the LC cell from the more standard transmissive type (*i.e.*, where the projection light is transmitted through the cell) to a reflective type. The main reason was that the operating wavelength of the GaAlAs lasers we used was $\approx$850 nm. This is considerably closer to the visible range than 1.06 μm, and we were not able to make ITO films which could absorb enough of the laser energy and still transmit white light. White-light projection is important for a multi-color version of the display. A second reason was that a transmissive LC cell requires a long working distance for the writing lens to allow for inserting the dichroic mirror used for simultaneous writing and projection of the LC cell.

A writing lens design with long working distance, high *NA*, and sufficient field coverage was determined to be difficult, hence expensive.

Although the use of a reflective cell solved the writing problems, it created new problems in projecting the cell onto a screen. It is more difficult to project an image of a reflective object than one of a transmissive object (this is fully explained in the next section). In addition, front-surface reflections from the cell limit the achievable contrast ratio (CR), and these reflections must be minimized. Even with an optimized cell, the maximum CR which can be obtained is less than that obtained with a simple transmissive cell.

A cross section of the reflective cell is shown in Fig. 7. As in earlier work [6], the cell is constructed with a Mylar spacer and is epoxy-sealed. The substrates are borosilicate glass with a thickness in the range of 1.5 to 2.3 mm. These glass plates, which have been ground and polished flat, are normally used for photomask substrates and are available with a surface flatness of 2 μm and in sizes up to 125 mm square. The front surface of the glass (as viewed from the projection side) has a multi-layer dielectric antireflection (AR) coating which reduces the reflection from 4% to $\approx$0.3%. The ITO transparent conductor has a resistance of $\approx$20 $\Omega/\square$; it is 137.5 nm thick. This is $\lambda/2$ at 550 nm (refractive index $n = 2$) and is chosen to minimize reflection [20]. The final coating is a narrow-band AR coating on the outside of the glass substrate, which eliminates the 4% reflection loss at the air/glass interface.

The purpose of the alignment layers is to give a preferred direction to the LC molecules in the neighborhood of the surface. These layers are SiO_2 and are created by evaporation or plasma deposition [21]. In contrast with earlier work [1–5] in which the surface treatment promoted homeotropic alignment (molecules normal to the surface), the alignment created is either homogeneous or random in-plane, depending on the method. The performance of the LC cell is highly dependent on these aligning forces, and a report on experiments designed to characterize this behavior will be published elsewhere [22]. In general, a strong homeotropic alignment tends to realign the written scattering texture. This gives excellent bulk-erase properties, but written spots tend to fade. At high enough bias temperatures the cell no longer has memory. In addition, the energy needed to write a spot is high. On the other hand, a strong in-plane alignment makes the erased state of the cell unstable. Written spots tend to bloom, and in severe cases, the cell spontaneously nucleates focal conic textures. These cells, however, have the lowest writing energy. There is clearly a compromise between these extremes which gives stable spots with low writing energy.

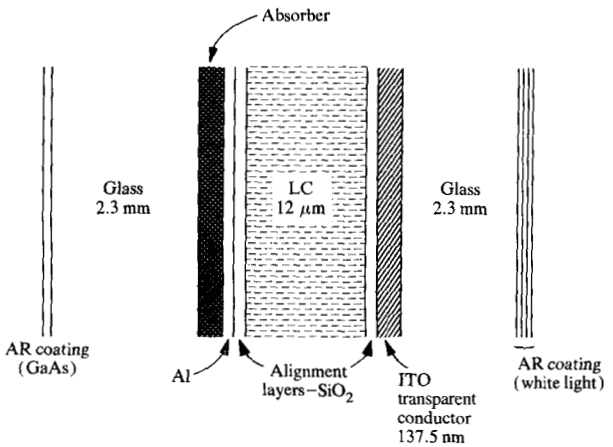

Figure 7 Reflective LLCD cell.

Another important factor in obtaining low writing energy is the design of the absorber/reflector layer. This layer should have high reflectivity of visible light on the LC side and high absorption of the GaAs laser energy, and should make efficient use of this absorbed energy in heating a small volume of LC. The reflectivity of the Al mirror is approximately 80%. This could be improved substantially by a multi-layer dielectric overcoat; however, the overcoat thickness would be several hundred nanometers thick, putting the absorber layer further from the LC.

Increasing the reflectivity of the cell improves the brightness and contrast ratio (CR) of the display, but this is not the major consideration. Of more importance is the 20% of the projection light absorbed by the cell. The temperature depends on the irradiance of the cell, which can be minimized for a given illuminance by using heat filters. Since the LC is biased at an elevated temperature, heating from the projection lamp is usually insignificant. In most of our work the cell has been biased to a temperature of 55–60°C, with an ambient temperature of 20–25°C. Care must be taken to avoid nonuniform irradiance of the cell, since a "hot spot" on the cell can cause undesirable writing effects. In most cases we found it desirable to control the temperature of the cell to within less than 1°C. The final coating shown in Fig. 7 is a narrow-band AR coating on the outside of the glass substrate. This eliminates the 4% reflection loss at the air/glass interface.

With an optimized reflective cell, a CR of 40:1 has been achieved with an f/11 projection system, and a spot size as low as 10 μm. The writing energy was <0.2 μJ/pel for a CR of 10:1. This writing energy is considerably lower than published results on transmissive cells.

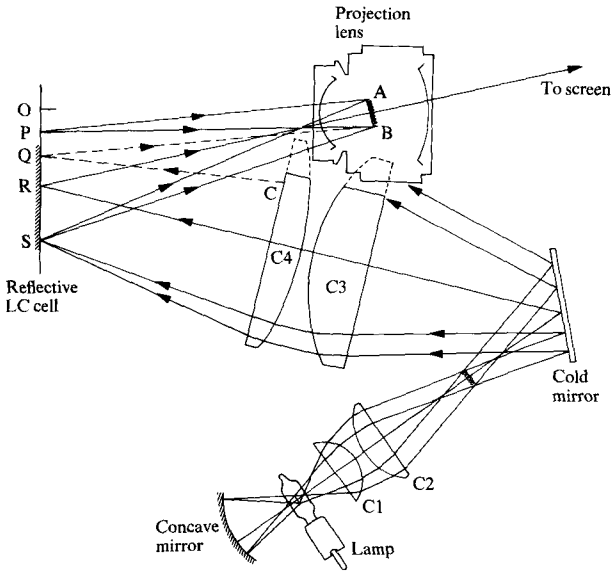

Figure 8 Off-axis projection system for the LLCD.

Projecting the LC image

The art of projecting a transmissive object is well established through the development of slide projectors, movie projectors, and microfilm viewers, etc. In the case of reflective objects, only one system comes to mind, the epidiascope, or "opaque projector." This system, which is used to project a reflective scattering object, typically a sheet of paper, floods the object with a great deal of light and uses the small fraction of this light that is collected by the projection lens to form an image on the screen. A study of projection systems [23] pointed out the difficulties in projecting a reflective light "valve," such as our LC cell, and classified projection systems according to the type of illumination.

The first experimental laser LC displays, which were built with reflective cells [20], used Class III reflex projection systems [23]. This type of system uses a telecentric projection lens which "collimates" the illuminating beam. It is essentially a folded version of the system shown in Fig. 1. The problem with a telecentric lens is that the diameter of the lens must be larger than the diameter of the LC cell. For small LC cells it was possible to use off-the-shelf lenses, but for larger cells (*i.e.*, approaching 125 mm square) a custom-designed telecentric lens would be necessary. An alternative projection approach is to use an off-axis Class I system [23], as shown in Fig. 8. The lens is a flat-field photographic enlarging lens which can adequately resolve the 40 line pairs/mm (lp/mm) on the LC cell, which corresponds to a pel size of 12.5 μm. The LC cell occupies only a small fraction of the nominal field of view of the lens. In our experimental LLCD, a 135-mm f/5.6 enlarging lens is used to project an LC cell of 25 × 32 mm. A larger LC cell would require a longer-focal-length lens, but we would have to maintain the resolution requirement to increase the number of resolvable pels on the screen. A practical upper limit to the size of the LC cell appears to be ≈125 mm square.

The illumination system of Fig. 8 has a relay condenser system in order to be able to use an inexpensive molded aspheric lens (C1 in figure). This lens is an efficient collector of light from the tungsten-halogen lamp. The projection system delivers an output in excess of 100 lumens from a 100-W lamp. Greater light output, for large-screen projection, would be possible with a Xe arc lamp as the light source.

Experimental display performance

The experimental LLCD used an eight-laser array, with individual lasers as shown in Fig. 4. The microprocessor-based system which provided the data to be displayed limited the x-scan velocity to 63 mm/s, or a dwell time of 200 μs. Because of the long dwell time, laser power was controlled at 5 mW for a 40-μs pulse. This enhanced the lifetime of our experimental lasers. With this writing energy (0.2 μJ per pel), a CR of 18:1 on the projection screen was achieved. The 25 × 32-mm LC cell allowed 2000 × 1760 spots to be addressed with 220 scans of the writing head. The line-writing speed of the LLCD was 4×10^4 (40K) pels/s, and the average writing speed, including the flyback time of the scanner, was 24K pels/s. In recent improvements to the system, bidirectional writing at a peak rate of 320K pels/s has been demonstrated.

On the basis of these results, we can project the writing speed achievable using an array of N lasers, each capable of delivering 10 mW to the cell. The pulse time is thus 20 μs and, assuming the laser is capable of a 100% duty cycle, we can make the dwell time 20 μs. Let us use, as an example, a display of 4000 × 4000 pels with a 50-mm-square LC cell. The time for one x-scan will be 4000 × 20 = 80 ms. If we allow 30 ms for decelerating and for accelerating the write head, this gives 60 ms for the stepping motor to move the y-scan. With bidirectional writing, the time per scan is thus 80 + 60 = 140 ms, and the writing speed is $4000N/0.14 = 36\,000N$ pels/s. With $N = 32$, the speed would be 1.16×10^6 (1.16M) pels/s, and the 16M-pel display would take 14 s to fully update. Clearly, the writing speed is determined by the laser power and the number of lasers. If a given update time is needed for an application with a specified laser lifetime, the laser power level, the number of lasers, and the cost of the lasers can be determined.

Conclusions

The viability of a GaAlAs injection-laser-addressed liquid-crystal cell for a projection display application has been demonstrated. The design trade-offs are such that both high

writing speed and high information content are possible, making the display attractive for many applications such as computer-aided design, document composition, or cartography. Present injection lasers can meet the performance and packaging requirements of the display, although there is still some concern about the laser's high-power reliability and commercial availability. The ability to use laser arrays for this display is still at an early stage of development, although this may be a cost-effective approach to multi-spot sources. The fiber optic delivery system gives the display designer flexibility in the type of lasers used and in the design of the scanning and imaging systems. The use of reflective LC cells has been demonstrated to give superior performance to the earlier transmissive cells, as well as offering very high information content, selective erase, and multi-color potential [24].

Acknowledgments

This project was the result of the contributions of many people, to whom we are deeply grateful. Contributions from the Thomas J. Watson Research Center mainly involved the laser and its delivery system, and include work of A. R. Benoric, M. J. Brady, C. B. Burstell, L. D. Comerford, J. S. Harper, H. C. Ifill, R. A. Laff, R. T. Lynch, R. M. Potemski, M. B. Small, and R. Tibbetts. Contributions from the San Jose Research laboratory involved the LC cell, the scanning and projection subsystems, and fabrication of prototype devices, and include work of J. Cockerill, A. Juliana, R. W. Koepcke, G. J. Sprokel, and C. E. Stratton. Finally, we want to acknowledge the inspiration, guidance, and technical contribution of our management, specifically R. C. Durbeck, R. Y. Hung, B. G. Huth, and E. G. Lean.

References and notes

1. F. J. Kahn, "IR-Laser-Addressed Thermo-Optic Smectic Liquid-Crystal Storage Displays," *Appl. Phys. Lett.* **22,** 111–113 (1973).
2. R. A. Heinz and R. C. Oehrle, "Rapid Generation of Complex Images with a Liquid Crystal," *Western Electric Engineer* **21,** 1–15 (1977).
3. M. Hareng, S. Le Berre, and L. Thirant, "Electric Field Effects on Biphenyl Smectic A Liquid Crystals," *Appl. Phys. Lett.* **25,** 683–685 (1974).
4. M. Hareng, S. Le Berre, and R. Hehlen, "Valve Optique à Crystaux Liquides Smectiques," *Revue Technique Thomson-CSF* **9,** 373–394 (1977).
5. M. R. Smith, R. H. Burns, and R. C. Tsai, "Ultrahigh-Resolution Graphic Data Terminal," *Proc. Soc. Photo-Optical Instrumentation Engineers (SPIE) Conf.* **200,** 171–178 (1979).
6. H. Melchoir, Frederic J. Kahn, D. Maydan, and D. B. Fraser, "Thermally Addressed, Electrically Erased, High-Resolution Liquid Crystal Light Valves," *Appl. Phys. Lett.* **21,** 392–394 (1972).
7. R. T. Lynch, Jr., M. B. Small, and R. Y. Hung, "GaAs/(GaAl)As Laser Technology," *IBM J. Res. Develop.* **23,** 585–595 (1979).
8. Robert T. Lynch, Jr., "Effect of Screening Tests on the Lifetime Statistics of Injection Lasers," *IEEE J. Quantum Electron.* **QE-16,** 1244–1247 (1980).
9. H. Imai, M. Morimoto, K. Hori, M. Takusagawa, and H. Saito, "Long-Lived High-Power GaAlAs DH Laser Diodes," *IEEE J. Quantum Electron.* **QE-16,** 248–250 (1980).
10. R. T. Lynch, Jr., IBM General Products Division Los Gatos laboratory, 5600 Cottle Rd., San Jose, CA 95193; unpublished work.
11. D. Botez, "Single Mode AlGaAs Diode Lasers," *J. Opt. Commun.* **1,** 42 (1980).
12. N. Chinone, K. Saito, R. Ito, and K. Aiki, "Highly Efficient [GaAl]As Buried-Heterostructure Lasers with Buried Optical Guide," *Appl. Phys. Lett.* **35,** 513–516 (1979).
13. Hisao Kumabe, Shigeyuki Nita, Yoshito Seiwa, Toshio Tanaka, Toshio Sogo, Shigeki Horiuchi, and Saburi Takamuya, "Continuous-Wave 15 mWatt Operation Test of Single-Mode High Power Crank Structure TJS Laser Diodes," *Proceedings of the Conference on Lasers and Electro-Optical Systems (CLEO'81), Paper FA 4,* Washington, DC, June 1981.
14. J. D. Crow, L. D. Comerford, J. S. Harper, M. J. Brady, and R. A. Laff, "Gallium Arsenide Laser-Array-on-Silicon Source Package," *Appl. Opt.* **17,** 479–485 (1978).
15. R. A. Laff, L. D. Comerford, J. D. Crow, and M. J. Brady, "Thermal Performance and Limitations of Silicon-Substrate Packaged GaAs Laser Arrays," *Appl. Opt.* **17,** 778–784 (1978).
16. Michael J. Brady, "Fabrication Processes for a Silicon Substrate Package for Integrated Gallium Arsenide Laser Arrays," *J. Electrochem. Soc.* **125,** 1642–1647 (1978).
17. J. D. Crow, D. L. Rogers, L. D. Comerford, A. X. Widmer, and P. A. Franaszek, "High Performance Fiber Optic Link for Computer Applications," *Proceedings of the 6th European Conference on Optical Communications (ECOC),* York, U.K., Sept. 1980, p. 450.
18. Located at the IBM Thomas J. Watson Research Center, Yorktown Heights, New York.
19. G. T. Sincerbox, "Thermal Writing Experiments with GaAs on a Liquid Crystal," *Research Report RJ-1969,* IBM Research Division laboratory, San Jose, CA, 1977.
20. A. G. Dewey, "Projection Storage Displays Using Laser-Addressed Smectic Liquid Crystals," *The Physics and Chemistry of Liquid Crystal Devices,* G. J. Sprokel, Ed., Plenum Press, New York, 1980, pp. 23–37.
21. G. J. Sprokel, "An RF Plasma Technique for Producing Twisted Nematic Liquid Cyrstal Cells," *op. cit.* Ref. 20, pp. 219–239.
22. D. Armitage and C. E. Stratton, "Surface Alignment and the Smectic Liquid Crystal Display," IBM Research Division laboratory, 5600 Cottle Rd., San Jose, CA 95193; unpublished results.
23. A. G. Dewey, "Projection Systems for Light Valves," *IEEE Trans. Electron Devices* **ED-24,** 918–929 (1977).
24. A. G. Dewey, "Image Overlay Using a Single Projection Lens," *IBM Tech. Disclosure Bull.* **21,** 1201–1202 (1979).

Received June 29, 1981; revised September 22, 1981

A. G. Dewey is located at the IBM Research Division laboratory, 5600 Cottle Road, San Jose, California 95193. J. D. Crow is located at the IBM Thomas J. Watson Research Center, P.O. Box 218, Yorktown Heights, New York 10598.